Characterising the phase behaviour of stearic acid and its triethanolamine soap and acid–soap by infrared spectroscopy

ARTICLE *in* PHYSICAL CHEMISTRY CHEMICAL PHYSICS · AUGUST 2009

Impact Factor: 4.49 · DOI: 10.1039/b819582j · Source: PubMed

3 AUTHORS:

Paul D A Pudney
Unilever
73 PUBLICATIONS **1,417** CITATIONS
SEE PROFILE

Kevin Mutch
Clariant International Ltd.
26 PUBLICATIONS **420** CITATIONS
SEE PROFILE

Shiping Zhu
Unilever
19 PUBLICATIONS **283** CITATIONS
SEE PROFILE

Characterising the phase behaviour of stearic acid and its triethanolamine soap and acid–soap by infrared spectroscopy

Paul D. A. Pudney,* Kevin J. Mutch and Shiping Zhu

Received 4th November 2008, Accepted 13th March 2009
First published as an Advance Article on the web 3rd April 2009
DOI: 10.1039/b819582j

The behaviour of stearic acid neutralised by triethanolamine to form soap and its acid–soap has been examined by infrared spectroscopy. It was found that not only could the neutralisation behaviour be characterised, but the thermotropic behaviour could also be followed. The neutralisation confirmed the formation of a fixed stoichiometeric ratio, 2 : 1, acid–soap. When following the thermotropic behaviour the break up of the acid–soap could be followed along with various disordering and melting transitions of the alkyl chain tail. This allowed all the thermal transitions that have been observed to be characterised in terms of the type of molecular rearrangement that was occurring and also the transition temperature at which they occurred. This allowed the binary phase diagram to be plotted and understood for this system. This is the first time IR has been used to measure a whole phase diagram of this type. The nature of the acid–soap complex itself was also characterised, with very short hydrogen bonds being present as well as a free, non-hydrogen bonded, hydroxyl group.

1. Introduction

The first allusion to acid–soaps was made by Chevreul in 1823,[1] and although their existence has often been disputed, there is now comprehensive proof.[2] These compounds are of great interest academically but also very important commercially, being found in superfatted, transparent and traditional soap bars, cleaning products, cosmetics, facial cleaners, shaving creams, deodorants and topical-delivered products.[2] Additionally these types of molecules are thought to be of biological importance.[3] Generally, acid–soap complexes are a group of molecular compounds that form as a consequence of a strong hydrogen bond between the fatty acid and its soap (carboxylate ion).[4] They consist of crystals containing carboxylic acid and, usually, metal carboxylate ions. The amount of these components is stoichiometrically discrete and are given by the general formula $M_xH_yA_z$ with X, Y and Z integers (X + Y = Z), M usually being the metal counter ion, mostly K^+ or Na^+[5–9] and A is the alkanoate ion of the form $CH_3(CH_2)_nCOO^-$ with *n* between 6 and 20.[2] This study differs in that the neutralisation is of stearic acid ($CH_3(CH_2)_{16}COOH$) by triethanol amine (TEA, $N(C_2H_4OH)_3$). There are very few studies published on amine soaps,[10] despite their wide use in the cosmetic industry where they are commonly used to replace alkali metal neutralised fatty acids.[11]

The conventional methods of studying these and similar lipid/fat systems are to use XRD to give crystallographic spacings and DSC to observe the thermal events during phase transitions. These methods usually allow a phase diagram to be produced; indeed recent work has used these methods for this stearic acid/TEA system.[10] FTIR has for many years been used to investigate the chemical state and interactions of carbonyl and carboxylate groups[12] and there is also an extensive literature on how alkyl chain behaviour can be studied using IR, including much work on fatty acids and soaps.[13,14] The polymorph of stearic acid can also be determined by IR spectroscopy.[15] It would therefore appear to be a good method to apply to acid–soap complexes, as has previously been observed by Lynch in his review on acid–soaps.[2] It should in principle be possible to characterise both the carbonyl/carboxylate head group behaviour and also that of the alkyl chains. There have been a limited number of FTIR studies on acid–soaps, which further highlight its usefulness; these mainly concentrate on the head group behaviour at ambient temperatures.[5] Two studies looked at acid–soaps and their thermotropic behaviour,[3,16] however doubt has been cast on the nature of the starting complexes due to the method of preparation.[2] Despite these doubts, this work showed that much information is available from the infrared spectra in particular: the intermolecular interactions between the acid and the soap as a function of the neutralisation degree and temperature, which are impossible or difficult for the conventional techniques such as microscopy, DSC and XRD which are used in construction of the binary phase diagram. Also, as the nature of the acid–soap itself is not totally understood, some further insights into this should be obtainable from the IR spectra.

It has recently been shown that neutralisation of stearic acid by TEA produces a stable 2 : 1 acid–soap complex and its thermotropic behaviour was explored.[10] Here we show in detail how a full range of neutralisations of stearic acid with TEA and their thermotropic behaviour can be understood by using FTIR. This is to see if insights that have been gained in studies by infrared spectroscopy in acid and lipid systems can be used to obtain further information for the type of systems under study here.

Unilever Discover, Colworth Science Park, Sharnbrook, Bedford, UK MK44 4LQ. E-mail: Paul.Pudney@unilever.com

2. Experimental

Stearic acid and triethanolamine (TEA) were provided by Fisher Scientific. The purity of stearic acid and TEA were 98% and 99% respectively. The neutralisation degree of stearic acid is calculated based upon the molar ratio of stearic acid to TEA and samples with different neutralisation degrees were prepared. These were, 5% (TEA), 13%, 20%, 25%, 33%, 40%, 50%, 60%, 70%, 80%, 85%, 90% and 100%. To prepare them, stearic acid was melted at 80 °C in a water bath and TEA was then added to the melt whilst being stirred. The temperature of the mix was then increased to 95 °C to obtain an isotropic solution. The solution was then cooled and solidified in an ambient environment. The resulting solid was ground down to form a powder. The powder was stored in a closed container for at least 7 days before it was analysed.

The infrared measurements were carried out using a Biorad (now Varian) FTS 6000 FTIR spectrometer. The samples were measured using a diamond ATR 'golden gate' with a uniform and reproducible covering of sample; as the ATR method measures the same volume above the surface (given the same refractive index), this implies a constant amount of sample is examined. The temperature was controlled using a heatable top-plate with a quoted temperature accuracy of 1 °C (Greasby Specac UK. Ltd). Spectra were taken at resolution of 2 cm^{-1} and each spectrum consisted of 256 scans co-added and ratioed against an air background spectrum. A series of background spectra were collected before each experiment according to the temperatures at which measurements were to be made. The correct background was then chosen to ratio against the sample spectra according to the temperature.

3. Results and discussion

3.1 Stearic acid and neutralisation with TEA

As the starting molecule for this study is stearic acid, its infrared spectrum from 600 to 3500 cm^{-1} is shown in Fig. 1 and the main observed bands, their frequencies and assignments with appropriate references are given in Table 1. The spectra from the fingerprint region of the resulting neutralisation of stearic acid to different degrees are shown in Fig. 2. A number of changes can be seen in the spectra, but the most diagnostic for acid–soaps are changes in the carbonyl/carboxylate region.[2,3,5] For clarity this region is shown in close up in Fig. 3. It can be seen that stearic acid

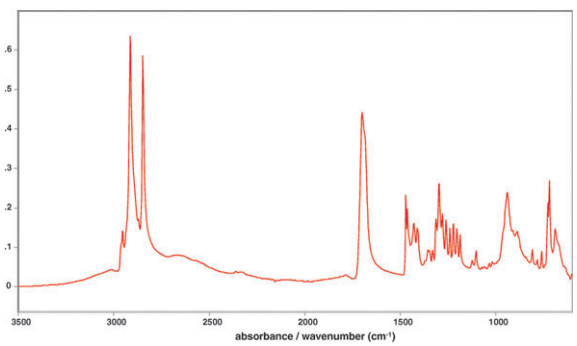

Fig. 1 Infrared spectrum of stearic acid at room temperature.

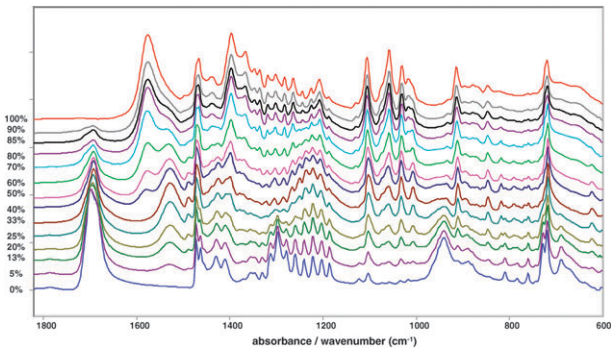

Fig. 2 Infrared spectra of the fingerprint region at room temperature of 100% TEA neutralised sample through to stearic acid (0% TEA neutralised). Spectra have been offset for clarity.

shows a carbonyl peak at 1698 cm^{-1} and shows no carboxylate peak (see later, 1575 cm^{-1} for the fully neutralised soap). This is expected as most fatty acids exist in dimeric form, hydrogen bonded to another fatty acid molecule and hence have no dissociated COOH groups.[17,18] The carbonyl band does have a low frequency shoulder, which is consistent with the stearic acid being in its most stable C crystal form. In this form, there is a *cis–trans* isomerisation around the C_1–C_2 bond (*i.e.* carbonyl carbon and the first carbon in the alkyl chain) and hence the carbonyl is in two different environments thus leading to the spilt into two bands. This is confirmed by the C═O in-plane deformation which also appears as a doublet at 690 cm^{-1} and 670 cm^{-1} due to *cis* and *trans* isomers respectively,[14,19–22] see Fig. 2.

The 100% neutralised sample shows a carboxylate peak at 1576 cm^{-1} as expected for the soap. However when TEA is added at 5% there is no band at 1575 cm^{-1} but a band appears at 1530 cm^{-1}. This is a similar frequency to that observed by Lynch *et al.*[6] for a 1 : 2 sodium palmitic acid–soap. As more TEA is added the carbonyl band decreases in intensity and shifts to a slightly lower frequency, typically 1692 cm^{-1}, whilst the carboxylate peak increases in intensity and also shifts to a slightly lower frequency. Above 33% however, the nature of the reaction changes; the further addition of TEA produces a band close to 1575 cm^{-1} due to the presence of soap. The lower frequency carboxylate peak due to acid–soap is still present and can still be observed when 90% TEA has been added.

Thus initially when stearic acid is neutralised it produces an acid–soap, giving a mixture of acid–soap and unreacted stearic acid. This continues until 33% after which soap is produced, giving a mixture of soap and acid–soap. As 33% is the critical point, this confirms other work[10] that the acid–soap complex consists of a 2 : 1 mixture of acid and soap. On plotting the intensity of the carbonyl band, $I_{C=O}$, there is a linear relationship between $I_{C=O}$ and the % TEA (not shown) and allows the direct deduction of the degree of neutralisation for any unknown sample, if so desired.

The observation of the frequency shifts provides information on the nature of the acid–soap complex. The carboxylate of the acid–soap is likely to be more hydrogen bonded than soap as the frequency is lower, similar to that observed previously. The carbonyl shows a lowering of the

Table 1 Band assignments

Wavenumber/cm^{-1}	Assignment	Strength
~688	O–C═O in plane angle deformation; SA, 5%, 13%, 20%, 25%[9,29,36]	m-np
~717	All in phase CH_2 rock; 33% and above[9,37]	vs
~719/728	Split all in phase CH_2 rock; SA, 5%, 13%, 20% and 25% (sh)[2,5]	vs
~760	CH_2 rock[36]	m-w
~783	CH_2 rock[36]	m-vw
~809	CH_2 rock[36]	m-w
~888	CH_3 rocking mode; SA, 5%, 13%, 20%[9,32,36,37]	m-w
~912	CH_2 rock[36]	m-s
~940	COH out of plane deformation (distinct up to 25%)[17,29,36]	vs-np
~1017	CH_2 rock[36]	vw
~1033	C–C stretch[36]	vw-s
~1058	Antisymmetric CH_2 rock: strong for high % (signifies 8 or more *trans*-CH in methylene chain)[34,38]	vw-s
~1104	Symmetric CH_2 rock with CH_3 sided chain[38,39]	m-s
~1123	C–C stretch[36]	w-np
~1129	Symmetric CH_2 rock with COO^- sided chain: only high% (16–20 or more t-CH)[36,38]	np-w
~1186–1348	CH_2 wagging progression[9,36]	s
~1297	Mostly C–OH stretch (SA, 5%, 13%, 20%)[17,29,36]	s-w
~1371	CH_3 symmetric deformation[18,27,36]	vw
~1378	CH_3 umbrella deformation[9,28]	np-vw
~1397	COO^- symmetric stretch-appears as shoulder for low %, not SA[9]	np-s
~1410	Bending of CH_2 adjacent to carboxyl group (α-CH_2)[28,29,36]	m-np
~1424–1430	C–O stretching and COH in plane bending (up to ~70%)[6,17,29,36]	m-np
~1439	COH in plane bending (25–60% sh, 70% -)[29]	np-w
~1462/1471	CH_2 scissor (up to 25%)[2,5]	s
~1467	CH_2 scissor (higher than 25%)[2,5]	m
~1528	COO^- antisymmetric stretch, acid–soap: all, but 100, 90, 85, 80 are sh[5,6]	w-m-sh
~1576	COO^- antisymmetric stretch, soap: only above 33%[5,6]	np-w-s
~1693	C═O high %[6]	w-np
~1698	C═O low %[6]	vs-w
~2848	CH_2 symmetric stretch[9,38,40,41]	vs
~2871	CH_3 symmetric stretch[9,38,40,41]	m
~2894	Fermi resonance[40,41]	sh
~2915	CH_2 antisymmetric stretch[9,38,40,41]	vs
~2932	Fermi resonance[40,41]	sh
~2953	CH_3 antisymmetric stretch (out of plane)[9,38,40,41]	m
2961	CH_3 antisymmetric stretch (in plane)[9,38,40,41]	w
High *T*		
~846	CH_3–CH_2 rocking mode for *tgttt* (high %)[32]	w
~1211	CH_2 wag; all except SA, 5%, 13%[32]	w
~1280	CH_2 wag; SA, 5%, 13%, 20% and 70%, 80%, 85%, 90%, 100%[32]	w
~1301	CH_2 wag-*gtg′* sequence: 40% @ 1297, 50% @ 1299, 70–100% @ 1301–1303[9,28,32,34,35]	w
~1340	CH_2 wag end-*tg* (*etg*) sequence; all, mainly shoulder for high%[9,28,32,35]	w
~1367	Out of phase CH_2 wag of *gtg′* sequences[9,28,32]	w

Abbreviations: *t* = *trans*; *g* = *gauche*; s = strong; m = medium; w = weak; v = very; sh = shoulder; np = not present; SA = stearic acid. Where strength assignments vary, the first is for low % TEA and the changes occur as % TEA increases.

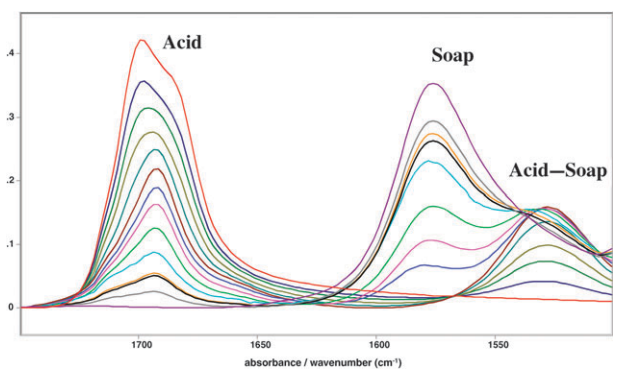

Fig. 3 The C═O (~1710 cm^{-1}) and COO^- stretching region (~1580 to 1530 cm^{-1}) for all samples at room temperature, labelled according to their origin, see text.

frequency from that of the acid alone, which is in contrast to the observation for the akali metal acid–soaps where the frequency was shown to increase.[3,6] Further information should be available from the ν OH, although this is complicated by the presence of OH groups in the cation. The full acid–soap complex spectrum is shown in Fig. 4. There are three distinct bands present above 3000 cm^{-1} for the acid–soap complex, the lowest of which is likely to be from the TEA counter ion. The band at approx. 3500 cm^{-1} is at the right frequency for a free OH in a carboxylic acid, suggesting one OH is sterically restricted from interacting. As the carbonyl peak suggests the presence of a hydrogen bonding interaction, the other OH should be observed as a broad band at lower frequency. Hydrogen bonded OH bands in carboxylic acids would normally be expected to occur well below 3000 cm^{-1}, but no significant broad band is observable in the spectrum displayed in Fig. 4.

In the acid–salts of carboxylic acids, the short chained equivalents of acid–soaps have been observed to have 'very short' hydrogen bonds.[23] These have been observed to give rise to extraordinary lowering of the frequency of the OH stretch.[24] Two types of these 'very short' and hence very strong

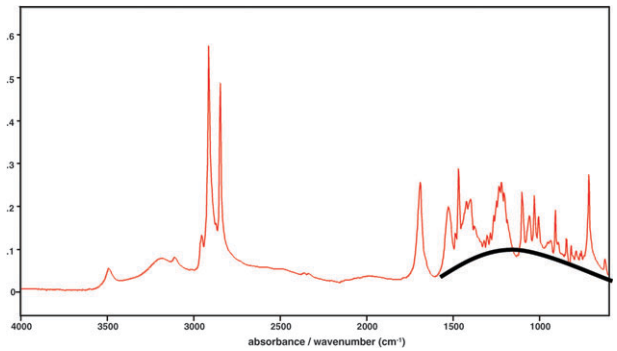

Fig. 4 FTIR spectrum of acid–soap. The black line shows location of possible underlying strong hydrogen bonded OH band.

hydrogen bonds have been classified by Speakman[23] as either type A or B, where the bonds are either symmetrical (*i.e.* the hydrogen is equidistant for the two oxygens) or unsymmetrical (where they are not). These show quite different IR spectral effects; a good summary of how the OH stretch changes with bonding distance and symmetry is given by Bratos.[25] Upon examining Fig. 4 it can be seen that there appears a very broad band underlying the spectrum from approximately 1600 cm^{-1} to below 700 cm^{-1} in the acid–soap, shown by an added black curve. A band of this type would also expect to have 'Evans holes' or windows,[26] but these would be extremely difficult to observe with so many other bands being present, although there are possible candidates which appear to be below the general level of background. A band structure of this type would be produced by nearly symmetrical hydrogen bonds with a length of 2.5 Å or below, *i.e.* very short and strong in nature. This corresponds well to the distance determined in $NaHP_2$ (P = palmitate) by X-ray diffraction of 2.44 Å.[6] The IR spectrum of this acid–soap was also shown, and it was suggested that the OH stretch is evident between 3000–2200 cm^{-1}, despite its presence not being obvious. However, an underlying broad band appearing largely in the fingerprint region could also be seen. This is consistent with a short hydrogen bond of the length suggested and hence we would assign this to the OH stretch. This was also observed and pointed out by Hadzi,[16] despite some concerns over the nature of these complexes.[2]

The vibrational spectroscopic work of Zerbi *et al.*[19] showed that the C form of stearic acid exists as a *trans* planar molecule with the carboxyl group co-planar with the chain, as has also been suggested by other authors.[14,27,28] This work demonstrates that, as is known for alkanes and other lipid systems, studying the carbon hydrogen vibrations of the methylene chains can tell you much about its conformation. Stearic acid, neutralised by 5%, 13% and 20% TEA, shows definite splitting of the in-phase CH_2 rock at 718 and 728 cm^{-1} (see Table 1 and Fig. 2). As the amount of TEA is increased, the intensity of the 728 cm^{-1} peak decreases until it is only a shoulder for 25% and is not observed for 33%, leaving only a single peak around 717 cm^{-1}. This splitting of the in phase rock indicates that the sample is crystalline with an orthorhombic sublattice.[29] The C form of stearic acid exists in a monoclinic form with the polymethylene chain comprising the sublattice of the orthorhombic type. These observations agree, as for low % TEA samples up until 33% there is still free stearic acid present, but as the amount of stearic acid decreases the degree to which splitting occurs also decreases. The similar splitting of the CH_2 scissor at 1462 cm^{-1} and 1472 cm^{-1} echoes the observation of the splitting of the CH_2 rock. Again, this is only observed clearly up to 20% and for 25% it is a shoulder. Thereafter this region shows only a single peak at 1467 cm^{-1}. This confirms the conclusion from the CH_2 rock behaviour.

3.2 Thermotropic behaviour

It is known that alkali *n*-alkanoates generally undergo more than one phase transition between a crystalline solid and isotropic liquid. The number of transitions depends on *n*, the number of carbon atoms; for members with $n > 6$, an anisotropic liquid phase (liquid crystal) is present before reaching the isotropic melt.[9] It is apparent therefore that for complex acid–soap structures, it can be expected that there will be more than one structural transition between solid and liquid. These type of phase diagrams have been described before[30,31] and are called peritectic. The transitions which are expected have been ascribed by DSC measurements for this system and are published in detail elsewhere.[10] The temperatures of the transitions observed in this previous work will be compared to the FTIR results described here. These different transitions in other fatty acid/soap/acid–soap systems have been found to be due to a number of different types of transition. These transitions have different effects on the head groups and the fatty acid chains and so different changes could be expected for vibrations originating from those parts of the molecules. Initially we will describe changes of vibrational modes from the head group and the fatty acid chains separately.

3.2.1 Fatty acid alkyl chains/C–H vibrations. Following on from the description above of the behaviour of the vibrations associated with the methylene chain with neutralisation, further changes would be expected with temperature, such as various melting and disordering/reordering phenomena. Thus this section will detail the observations that have been made on the various CH vibrations and how they can be used to clearly characterise the changes that occur in the fatty acid methylene chains with temperature.

On heating, the fatty acid chains generally change in conformation, often losing their ordered structure with the introduction of *gauche* bonds and rotation of the end methyl group. The effect of these changes should be primarily on the spectral regions dealing most clearly with the C–H bonds. There is much work in the literature describing vibrational spectroscopy on this type of change, mostly developed from the seminal work of Snyder.[32]

3.2.1.1 CH stretching region. It is known that the main C–H stretching region between 2800 and 3000 cm^{-1} yields information about the degree of disorder in the structure.[33] Some changes were observed in this region with neutralisation. Observing the CH_2 symmetric stretch for all samples at room temperature, it was noted that there is no systematic correlation between the amount of TEA present and the

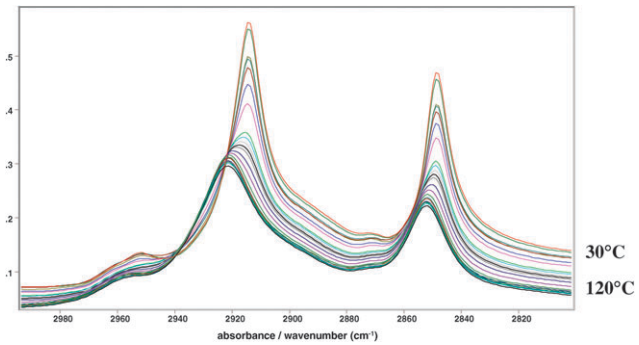

Fig. 5 The main C–H spectral region as measured for 85% TEA on increasing temperature. Showing how the CH_2 bands shift and broaden as the alkyl chain goes through a disordering/melting transition.

intensity of this peak. Although a gradual decrease in intensity as the amount of TEA increases was observed, it was not a linear relationship. The exact frequency of this peak was observed to increase until 40% TEA, whereby it reaches a maximum and then begins to decrease again. This band was observed for all samples with increasing temperature, with changes being taken relative to those at room temperature. An example of the typical behaviour observed is shown in Fig. 5, displaying the C–H stretching region for 85% TEA. It can be seen that along with a gradual decrease in intensity, there is also a shift to higher frequency as the temperature increases. This occurs smoothly until it reaches a critical point, *i.e.* a temperature at which a transition occurs, whereby it undergoes a large change. The shift of the frequency of the symmetric CH stretch peak at $\sim$2850 cm^{-1} was plotted and is shown in Fig. 6. Similar plots were obtained for all of the samples.

It can be clearly seen from Fig. 6 that there is more than one gradient change between the lower and higher frequency regions (from $\sim$2848.5 cm^{-1} to $\sim$2852 cm^{-1}), showing that at least two transitions are involved. The temperature at which these changes occur was obtained by taking the midpoint of the two lines involved. A third change can be observed on the higher temperature part and is discussed below, but it is not clear in this plot. For stearic acid, 25%, 33% and 40%, one transition was clearly observed. For 5%, 13%, 20%, 50% and 100% there were two clear transitions, and for the remaining compositions (60%, 70%, 80%, 85% and 90%) there were

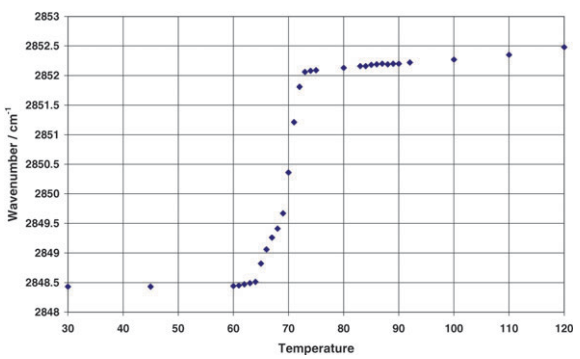

Fig. 6 Plot of the CH_2 symmetric band frequency for 85% TEA sample, as shown in Fig. 5, with increasing temperature.

three. A similar form has been observed for some alkali metal acid–soaps, but the origin of the transitions was not fully identified.[3] The origin of these transitions is due to disordering and/or melting, however to determine the precise nature of the different transitions, these changes need to be considered in conjunction with the observations of the head group vibrations.

Looking at the other C–H vibrations, it is clear that the CH_2 bend and CH_2 scissors both reflect the transitions for low% TEA samples. As was mentioned, these bands both show factor group splitting for stearic acid and the 5%, 13% and 20% TEA samples due to the orthorhombic packing of the polymethylene chains. On heating, the peak at higher frequency begins to decrease in intensity around the temperature of the first transition and is not observed at all when it is an isotropic liquid. This also reflects the disordering of the polymethylene chain which results in the break up of the orthorhombic packing.

3.2.1.2 C–H wagging region: 1150–1350 cm^{-1}. One of the regions which is of most interest in understanding structural changes is between about 1150 and 1350 cm^{-1}. This series of bands arises due to the methylene wag. Chapman concluded that the number of bands in the series is half the number of CH_2 groups in the acid chain.[13] The wag arises when all of the H atoms of the CH_2 groups move in the same direction along the whole chain and this in phase bend gives rise to the series which is observed. The wagging progression is much stronger in fatty acids than in the corresponding hydrocarbons for two reasons. Firstly, CH_2 waggings are strongly coupled with the motions of the C═O and C–O bonds which contribute significantly to the changes in the transition moments, and secondly, the carboxyl group induces a strong polarity of the C–C bonds along the chain; this polarity decreases as the distance from the carboxyl group increases. This makes the wagging much stronger for acids than the virtually non-polar hydrocarbons. [13] Not all the bands in this region arise from the wags; the origins of some of the others are documented in Table 1.

As the substances are heated, the methylene groups of the long fatty acid chains begin to change conformation such that they are no longer all *trans*. As this all *trans* structure is broken up, it causes the discrete methylene wagging structure in the spectra to lose its form, as it relies on the coupling between the vibrations of adjacent methylene groups. As the temperature is increased, the degree of disorder in these chains increases. Hence, the methylene wagging structure is no longer apparent in the spectrum as the isotropic liquid is reached. Instead, this is replaced by a number of very small bands which arise from other conformations of the acid chain (as assigned in Table 1).

New bands are observed at $\sim$1211 cm^{-1}, $\sim$1280 cm^{-1}, $\sim$1301 cm^{-1}, $\sim$1340 cm^{-1} and $\sim$1367 cm^{-1} as the samples are heated. These bands are not uniformly present for all of the samples, sometimes being of too small intensity or being masked by other larger peaks. The band found around 1301 cm^{-1} has been suggested as arising from the in phase wagging motion of the two CH_2 groups involved in the *gauche–trans–gauche′* (*gtg′*) conformation. Similarly, the band around 1367 cm^{-1} is the out of phase form of this vibration.[24]

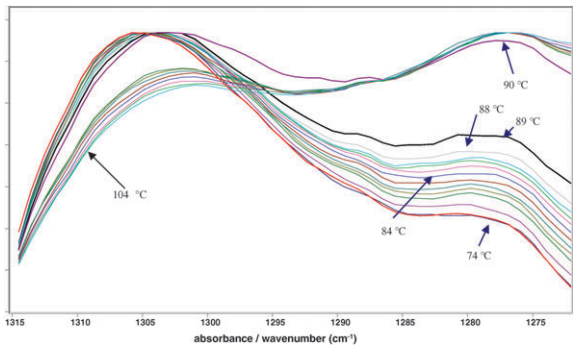

Fig. 7 Shows the changes in the bands at 1301 cm^{-1} and 1276 cm^{-1} for 85% TEA between 74 °C and 104 °C.

The same authors suggest that the mode near 1340 cm^{-1} is caused when the CH_2 group adjacent to the terminal CH_3 group is placed between a *trans* and a *gauche* conformation (end *tg*, *etg* group). The bands at around 1211 cm^{-1} and 1280 cm^{-1} have been attributed to C–C–C bending and methylene wagging, respectively[34] although the exact conformations giving rise to these is unknown.

On observing the spectra at higher temperatures, it is clear that the frequency behaviour of the band at approximately 1301 cm^{-1}, correlates to the weak transition that was observed at the higher temperature in the CH stretch region. This is the change upon going from liquid crystal to isotropic liquid phases. Plotting this change allows an observation to be made about the temperature of the transition. It is also observed that in the liquid crystal phase, the peak at 1301 cm^{-1} is generally more intense than the adjacent peak at 1276 cm^{-1}, as shown in Fig. 7 for 85% TEA. Upon melting however, the reverse is true. A plot of I_{1301}/I_{1276} is shown in Fig. 8, making the phase transition much clearer to observe, and thus allowing the transition temperature to be determined more accurately.

3.2.1.3 Other bands revealing heating phenomena. Although the main bands that were used in determining the temperatures of transition have been described, it is useful to look at bands which may uncover some further details about the structure of these compounds.

Work by Snyder and co-workers detailed the degree of conformational disorder of waxes by comparing the intensities of two bands at 1341 cm^{-1} and 1375 cm^{-1}.[35] These bands were assigned as being the CH_3 umbrella deformation (1375 cm^{-1})

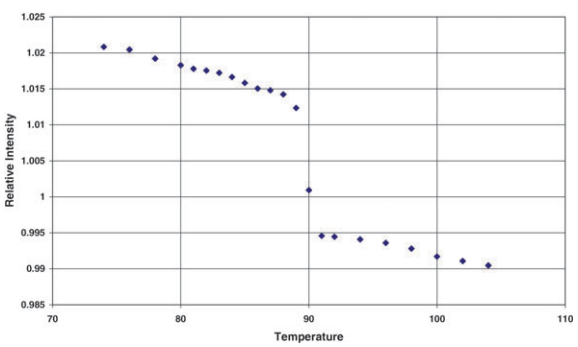

Fig. 8 Plot of 1301 cm^{-1} band intensity relative to 1276 cm^{-1} band for 85% TEA, *i.e.* I_{1301}/I_{1276}.

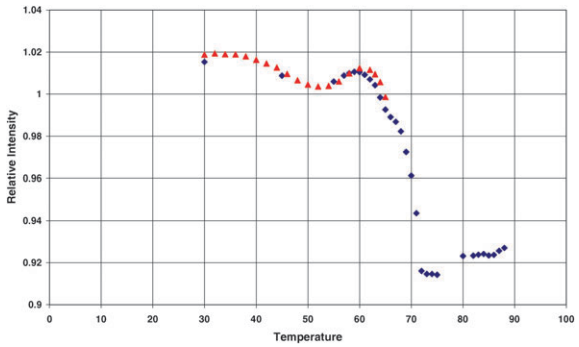

Fig. 9 Plot of intensity of the 1367 cm^{-1} band relative to the 1378 cm^{-1} band, I_{1367}/I_{1378}, for 80% TEA with diamonds being initial measurements and triangles repeated low temperature measurements.

and a methylene wag arising from an end *trans–gauche* sequence (1341 cm^{-1}). In this case however, it is not possible to observe the band at 1341 cm^{-1} for low temperatures because this is obscured by the main CH_2 wagging progression. There is a band at 1367 cm^{-1} however which, according to Snyder,[32] indicates a *gtg′* sequence. This band is out of the region of the CH_2 wag and hence is not obscured. The relative intensities of these changes with temperature can be determined by examining the spectra (not shown). The CH_2 *etg* band will be affected considerably by temperature, whereas the CH_3 umbrella will be affected differently as it is less strongly coupled to the adjacent groups/alkyl chain. Fig. 9 shows a plot of the relative intensities—I_{1367}/I_{1378}.

This graph shows a decrease in the intensity ratio between about 60 °C and 68 °C. The midpoint of this decrease is approximately 64 °C which agrees well with the previous observation (see Table 3). The next major change is between 69 °C and 72 °C and the midpoint of this is 70 °C, also in good agreement. For the higher temperature transition, the change is less clear. However, given the knowledge that there is a transition taking place around 86–87 °C, it can be seen that at this point in the above graph there is a slight increase in the relative intensity, which indicates a transition. Thus the plot of the relative intensities of the 1378 cm^{-1} and 1367 cm^{-1} bands does allow the prediction of all transitions taking place; it confirms the behaviour observed and gives further information about the type of disorder processes taking place.

3.2.2 Head group vibrations. Interesting deductions can be made about the shift of the carbonyl and carboxylate peaks on heating. As mentioned previously (Table 1) the peak occurring around 1700 cm^{-1} is due to the carbonyl group, the peak at 1530 cm^{-1} arises from the carboxylate groups of the acid–soap complex and the peak around 1575 cm^{-1} is due to the carboxylate groups of free soap.

On heating stearic acid to 68.5 °C, whereupon it melts, its carbonyl peak shifts by 12 cm^{-1} to 1710 cm^{-1}. This is due to the fact that in its crystalline form the acid exists dimerised to another stearic acid molecule, but on melting this association is less ordered, leaving more electron density in the C=O bond and hence making it stronger.[6] The effect is also observed for all the samples below 33%: the carbonyl peak always shifts to approximately 1710 cm^{-1} upon melting. The overall shift is

Table 2 Transitions occurring in acid–soap complexes

Sample	Transition	Peak used
Stearic acid	Acid/liquid	2850 cm^{-1} (CH_2 symmetric)
5%–25%: 1st transition	Acid–soap/acid	2850 cm^{-1} and carboxylate
5%–25%: 2nd transition	Acid/liquid	2850 cm^{-1}
33%	Acid–soap/liquid	2850 cm^{-1}
40%–90%: 1st transition	Acid–soap/soap	1710 cm^{-1} (C═O) and 2850 cm^{-1} and carboxylate
40%–90%: 2nd transition	Soap/liquid crystal	2850 cm^{-1}
40%–90%: 3rd transition	Liquid crystal/liquid	1301/1276 cm^{-1} (CH_2 wags)
100%: 1st transition	Soap/liquid crystal	2850 cm^{-1}
100%: 2nd transition	Liquid crystal/liquid	1301/1276 cm^{-1}

larger however, given the lower frequency of the band initially (approx. 1693 cm^{-1}).

The carbonyl group of the acid occurs at 1697 cm^{-1} and the same group for acid–soap is typically 1692–1693 cm^{-1}. It is expected that if the acid–soap goes to acid, the carbonyl peak will shift from 1693 cm^{-1} to 1697 cm^{-1} to reflect the changing environment. It would then shift to 1710 cm^{-1} on going to the isotropic liquid. It was observed that the carbonyl peak does not shift to the final frequency 1710 cm^{-1} until total melting has occurred and it changes from the acid–soap to acid, with the acid melting occurring separately.

It is observed that the carboxylate peak of the acid–soap, acid mixtures also change on heating. The carboxylate group shifts considerably at the same temperature of the carbonyl shift. For 5% TEA the shift is from 1530.2 cm^{-1} to 1554.8 cm^{-1}. On complete melting, it then decreases considerably in intensity although it does not change its position. This shift in frequency is explained by the changing environment of the carboxylate group. Thus when acid and acid–soap are present, it can be seen on melting that the acid–soap complex breaks up. This is shown by the frequency shift of the carboxylate band to a frequency similar to that observed for the soap, with only bands from the acid and soap observed. Similar changes are observed for all the samples up to 33%.

For the samples of above 33% TEA, the typical behaviour of the carboxylate region is shown in Fig. 10 (for 50% TEA). The acid–soap carboxylate peak at 1530 cm^{-1} and the soap band at 1580 cm^{-1} merge into one at just under 1560 cm^{-1}. Thus the acid–soap appears to be breaking up at this temperature. Simultaneously the carbonyl peak shifts up to around 1713 cm^{-1}, as was observed below 33% when both the acid–soap breaks up and the acid melts. However, unlike previously, this is not observed at the temperature at which the isotropic liquid is reached, as judged from the CH vibrations described earlier, although a disordering transition is observed. The transition is thus due to acid–soap breaking up, producing acid in the liquid state and soap. A further disordering (*i.e.* melting) of the soap is observed at a higher temperature, producing the isotropic liquid consisting of both acid and soap.

A plot of the shift of the carbonyl band can be used to measure the temperature of the transitions that are occurring, as shifts of the carbonyl band are observed for both the acid–soap break up to soap and acid and the acid melting transitions. An example of such a plot of the shift of this band is given for 85% TEA in Fig. 11.

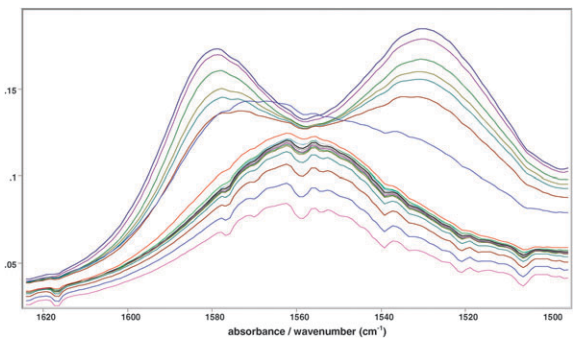

Fig. 10 Acid–soap (~1530 cm^{-1}) and soap (~1580 cm^{-1}) COO^- peaks on heating for 50% TEA sample. Room temperature spectrum at the top and highest temperature spectrum at the bottom.

Thus to summarise the observations above for both the head group vibrations and the tail/CH vibrations, it has been shown that all of the changes that occur for the acid/acid–soap/soap phase diagram as identified previously[10] can be observed in the infrared spectra. These are acid melting to liquid, acid–soap break up to acid and soap, acid–soap to liquid, soap to liquid crystal and liquid crystal to isotropic liquid. Also, as a lot of these changes show sharp temperature transitions, they can be used to measure the temperature at which they occur. This has been done in this study using the most appropriate bands often in combination with another band to confirm the type of transition that is occurring. The bands that have been used are summarised in Table 2. The temperatures obtained can then be used to plot the phase

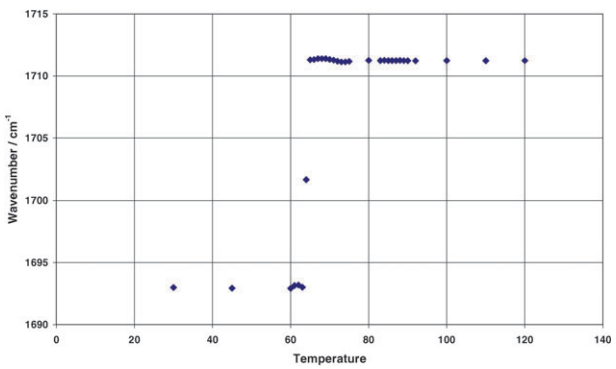

Fig. 11 Shift of the C═O band frequency for 85% TEA with increasing temperature, change due to the acid–soap to liquid acid transition, see text.

Table 3 Values obtained for transition temperatures

% TEA	Acid/liquid	Acid–soap/acid	Acid–soap/liquid	Acid–soap/soap	Soap/liquid crystal	Liquid crystal/liquid
0	68.5 °C					
5	67.6 °C	65.0 °C				
13	67.2 °C	65.7 °C				
20	67.0 °C	65.5 °C				
25	65.5 °C	65.5 °C				
33			66.5 °C			
40				66.5 °C	66.5 °C	
50				66.5 °C	67.0 °C	73.5 °C
60				65.5 °C	69.0 °C	75.0 °C
70				64.5 °C	69.0 °C	83.5 °C
80				64.3 °C	69.5 °C	89.0 °C
85				64.0 °C	70.5 °C	89.5 °C
90				61.5 °C	71.5 °C	91.0 °C
100					71.8 °C	91.5 °C

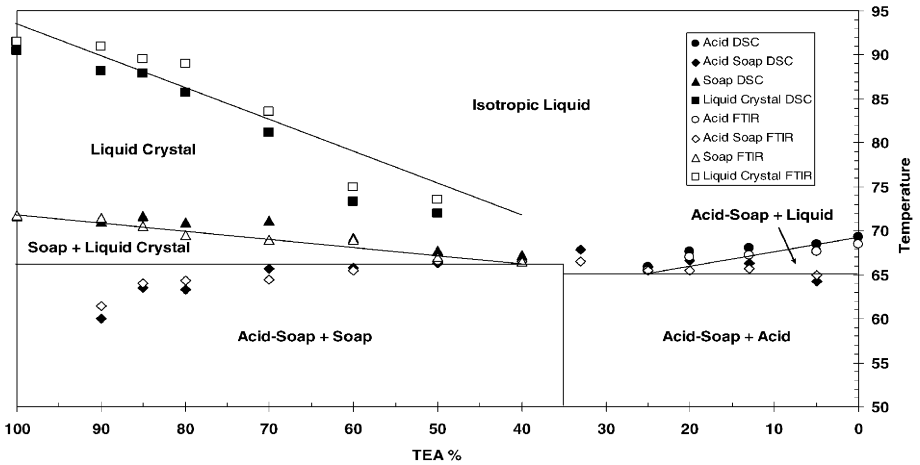

Fig. 12 Comparison of the phase diagram changes obtained from FTIR (open symbols) and DSC (filled symbols). Lines demarcating the approximate phase regions are also drawn, and the appropriate regions labelled.

diagram. The plot of this phase diagram is shown in Fig. 12, with the temperatures for the transitions given in Table 3. These values compare very well to those obtained by DSC measurements,[10] which are also plotted in the same Figure. However the DSC measurements of course do not unambiguously give the type of transition that is occurring.

4. Conclusions

This investigation has shown that infrared spectroscopy is a very good method for investigating phase behaviour and structural changes of stearic acid and its neutralisation products. This is the first time that such a detailed phase diagram has been constructed of such a system using FTIR spectroscopy. It is a quick and robust method that is sensitive to all the states encountered in the phase diagram. It was shown that it could not only distinguish between them, but it can give a detailed understanding of the local molecular environment. This was done by monitoring the changes of multiple bands from vibrational modes originating in both the 'head' group and the 'tail', the alkyl chain. Thus the neutralisation of stearic acid could be followed, showing the formation of both the acid–soap complex and the soap. The thermotropic behaviour was also characterised in detail. This shows, for instance, when the acid–soap complex breaks up and when various disordering/melting transitions of the alkyl chain take place, ultimately resulting in the formation of an isotropic liquid. The temperatures at which all these transitions occur could be measured accurately, matching well those obtained previously by DSC. Further insights into the nature of the acid–soap complex itself have been garnered. It has been shown to possess very short, strong, hydrogen bonds and a 'free', non-hydrogen bonded, OH group.

Acknowledgements

Mary Hepenstall-Butler for useful discussions and Professor Norman Sheppard FRS for discussions especially about the nature of the acid–soap.

References

1 M. E. Chervreul, *Recherches Chimiques sur les Corps Gras d'Origine Animales Paris*, 1923, **34**(53), 408.
2 M. L. Lynch, *Curr. Opin. Colloid Interface Sci.*, 1997, **2**, 495–500.
3 H. H. Mantsch, S. F. Weng, P. W. Yang and H. H. Eysel, *J. Mol. Struct. (THEOCHEM)*, 1994, **324**, 133–141.
4 P. Tandon, S. Raudenkolb, R. H. H. Neubert, W. Rettig and S. Wartewig, *Chem. Phys. Lipids*, 2001, **109**, 37–45.

5 M. L. Lynch, Y. Pan and R. G. Laughlin, *J. Phys. Chem.*, 1996, **100**, 357–361.
6 M. L. Lynch, F. Wireko, M. Tarek and M. Klein, *J. Phys. Chem. B*, 2001, **105**, 552–561.
7 J. Bian, S. F. Weng, J. G. Wu, L. Q. Yang, X. Zhang and G. X. Xu, *Mikrochimica Acta*, 1997, 367–368.
8 T. Ishioka, *Bull. Chem. Soc. Jpn.*, 1991, **64**, 2174–2182.
9 M. V. Garcia, M. I. Redondo and J. A. R. Cheda, *Vib. Spectrosc.*, 1994, **6**, 301–308.
10 S. Zhu, M. Heppenstall-Butler, M. F. Butler, P. D. A. Pudney, D. Ferdinando and K. J. Mutch, *J. Phys. Chem. B*, 2005, **109**, 11753–11761.
11 J. Falbe, *Surfacants in Consumer Products*, Springer-Verlag, Berlin, 1988.
12 L. J. Bellamy, *Infrared Spectra of Complex Molecules*, John Wiley, 1975.
13 D. Chapman, *The Structure of Lipids*, Methuen and Co. Ltd., London, 1965, ch. 4, p. 52.
14 M. Kobayshi, in *Crystallization and Polymorphism of Fats and Fatty Acids*, ed. N. Garti and K. Sato, Marcel Dekker, 1988, ch. 4, p. 139.
15 S. Zhu, P. D. A. Pudney, M. Heppenstall-Butler, M. F. Butler, D. Ferdinando and M. Kirkland, *J. Phys. Chem. B*, 2007, **111**, 1016–1024.
16 D. Hadzi, A. Grdadolnik and A. Meden, *J. Mol. Struct. (THEOCHEM)*, 1996, **381**, 9–14.
17 D. Hadzi and N. Sheppard, *Proc. R. Soc. London*, 1952, **216**, 247–266.
18 P. J. Corish and D. Chapman, *J. Chem. Soc.*, 1957, 1746–1751.
19 G. Zerbi, G. Minoni and A. P. Tulloch, *J. Chem. Phys.*, 1983, **78**, 5853–5862.
20 S. Hayashi and J. Umemura, *J. Chem. Phys.*, 1975, **63**, 1732–1740.
21 J. Umemura, *J. Chem. Phys.*, 1978, **68**, 42–48.
22 S. Hayashi, J. Umemura and R. Nakamura, *J. Mol. Struct. (THEOCHEM)*, 1978, **69**, 123–136.
23 J. C. Speakman, *Struct. Bonding*, 1972, **12**, 141–199.
24 D. Hadzi and B. Orel, *J. Mol. Struct. (THEOCHEM)*, 1973, **18**, 227–239.
25 S. Bratos, H. Ratajczak and P. Viot, *Properties of H-Bonding in the Infra red Spectral Range in Hydrogen Bonded Liquids*, ed. J. C. Dore, T. Teixiera, 2000, Nato Series C, vol. 329, pp. 221–35.
26 M. F. Claydon and N. Sheppard, *Chem. Commun.*, 1969, 1431–1433.
27 R. G. Sinclair, A. F. McKay and R. Norman Jones, *J. Am. Chem. Soc.*, 1952, **74**, 2570–2575.
28 M. Delzoppo and G. Zerbi, *Polymer*, 1990, **31**, 658–662.
29 G. Zerbi, G. Conti, G. Minoni, S. Pison and A. Bigotto, *J. Phys. Chem.*, 1987, **91**, 2386–2393.
30 D. M. Small, *The Physical Chemistry of Lipids*, Phenum Press, 1986, p. 332.
31 R. G. Laughlin, *The Aqueous Phase Behaviour of Surfacants*, Academic Press, 1994, p. 472.
32 R. G. Snyder, *J. Chem. Phys.*, 1967, **47**, 1316–1360.
33 A. Watkinson, R. S. Lee, A. E. Moore, P. D. A. Pudney, S. E. Paterson and A. V. Rawlings, *Int. J. Cosmet. Sci.*, 2002, **24**, 151–161, and references therein.
34 T. Ishioka, *Bull. Chem. Soc. Jpn.*, 1991, **64**, 2174–2182.
35 D. Clavell Grunbaum, H. L. Strauss and R. G. Snyder, *J. Phys. Chem. B*, 1997, **101**, 335–343.
36 R. F. Holland and J. Rud Nielsen, *J. Mol. Spectrosc.*, 1962, **9**, 436–460.
37 G. S. Yu, H. W. Li, F. Hollander, R. G. Snyder and H. L. Strauss, *J. Phys. Chem. B*, 1999, **103**, 1046–10468.
38 P. Tandon, S. Raudenkolb, R. H. H. Neubert, W. Rettig and S. Wartewig, *Chem. Phys. Lipids*, 2001, **109**, 37–45.
39 P. Tandon, R. H. H. Neubert and S. Wartewig, *J. Mol. Struct. (THEOCHEM)*, 2001, **526**, 49–57.
40 S. Abbate, G. Zerbi and S. L. Wunder, *J. Phys Chem.*, 1982, **86**, 3140–3149.
41 H. Binder and H. Schmiedel, *Vib. Spectrosc.*, 1999, **21**, 51–73.

